Inorganic Chemistry

Article

pubs.acs.org/IC

Copper(I)-α-Synuclein Interaction: Structural Description of Two Independent and Competing Metal Binding Sites

Francesca Camponeschi,[†] Daniela Valensin,*[,†] Isabella Tessari,[‡] Luigi Bubacco,[‡] Simone Dell'Acqua,[§] Luigi Casella,[§] Enrico Monzani,[§] Elena Gaggelli,[†] and Gianni Valensin[†]

[†]Department of Biotechnology, Chemistry and Pharmacy, University of Siena, Via A. Moro 2, Siena, Italy

[‡]Department of Biology, University of Padova, Via U. Bassi 58b, Padova, Italy

[§]Department of Chemistry, University of Pavia, Via Taramelli 12, Pavia, Italy

Supporting Information

ABSTRACT: The aggregation of α-synuclein (αS) is a critical step in the etiology of Parkinson's disease. Metal ions such as copper and iron have been shown to bind αS, enhancing its fibrillation rate in vitro. αS is also susceptible to copper-catalyzed oxidation that involves the reduction of Cu^{II} to Cu^{I} and the conversion of O_2 into reactive oxygen species. The mechanism of the reaction is highly selective and site-specific and involves interactions of the protein with both oxidation states of the copper ion. The reaction can induce oxidative modification of the protein, which generally leads to extensive protein oligomerization and precipitation. Cu^{II} binding to αS has been extensively characterized, indicating the N terminus and His-50 as binding donor residues. In this study, we have investigated αS−Cu^{I} interaction by means of NMR and circular dichroism analysis on the full-length protein ($αS_{1-140}$) and on two, designed *ad hoc*, model peptides: $αS_{1-15}$ and $αS_{113-130}$. In order to identify and characterize the metal binding environment in full-length αS, in addition to Cu^{I}, we have also used Ag^{I} as a probe for Cu^{I} binding. Two distinct Cu^{I}/Ag^{I} binding domains with comparable affinities have been identified. The structural rearrangements induced by the metal ions and the metal coordination spheres of both sites have been extensively characterized.

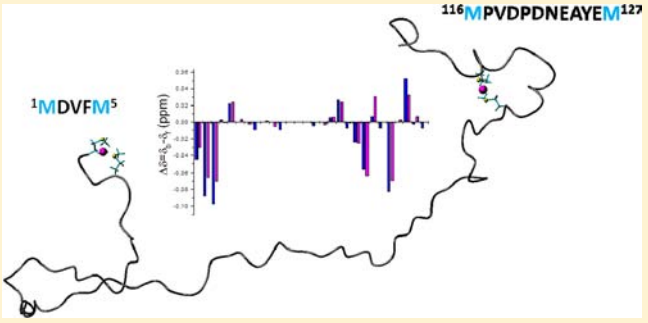

INTRODUCTION

Parkinson's disease (PD) is a devastating progressive neurodegenerative disease whose major clinical symptoms are tremors, movement impairments, postural instability, gait difficulty, and rigidity. PD is characterized by the loss of dopaminergic neurons[1,2] and by the presence of intracellular proteinaceous inclusions (Lewy bodies) mainly consisting of aggregated forms of α-synuclein (αS).[3−5]

αS is a 140-amino acid presynaptic protein of still unknown function. It is constituted by three different domains: (i) the amphipathic N terminus comprising the first 60 residues, (ii) the nonamyloidogenic component (NAC), highly hydrophobic and encompassing residues between 61 and 95, and (iii) the acidic C-terminal region (96−140) rich in Glu and Asp residues. αS is classified as an intrinsically disordered protein,[6,7] but it undergoes dramatic conformational transitions from its natively unstructured state to α-helix-rich conformations upon interaction with lipid membranes.[8,9]

In addition to the formation of αS aggregates, metal-induced oxidative stress and the directly or indirectly related formation of reactive oxygen species (ROS) have also been implicated in the pathogenesis of PD and other neurodegenerative diseases.[1,10] ROS can damage cells at different levels by causing (i) lipid membrane peroxidation,[11] (ii) oligomerization and/or inactivation of oxidized proteins, and (iii) cleavage of DNA and RNA molecules. The formation of ROS is accelerated in the presence of redox-active metals such as copper and iron,[12] and there is much evidence that abnormal metal homeostasis has a significant impact on the development of age-related neurodegenerative diseases.[13−15]

αS, like other proteins associated with neurodegeneration (Aβ, prion protein, etc.), interacts with copper, which can modulate αS aggregation and oligomerization.[16,17] Copper is an essential trace element and is a key component of many important enzymes involved in vital biochemical processes, such as iron acquisition, respiration, and free-radical detoxification.[18] On the other hand, high cellular levels of copper may result in toxicity for the cell. The toxicity has been attributed to Cu^{I}/Cu^{II} redox cycling, which leads to the production of ROS through Haber−Weiss or Fenton reactions.[19] To prevent metal-catalyzed oxidative stress, cells have developed sophisticated systems for copper storage and transport. An imbalance in copper homeostasis has been associated with genetic disorders such as Menkes disease and

Received: September 21, 2012
Published: January 23, 2013

   dx.doi.org/10.1021/ic302050m | *Inorg. Chem.* 2013, 52, 1358−1367

Wilson syndrome but also with neurodegenerative and prion diseases.[20]

It has been shown that αS, as well as the Aβ peptide, is highly susceptible to copper-catalyzed oxidation by ROS.[21−23] The reaction requires the ability of the protein to bind both Cu^{II} and Cu^{I} ions and leads to oligomerization and precipitation of the protein itself.[24] Cu^{II} complexed by both full-length αS and its N-terminal fragment αS_{1-19} can be reduced to Cu^{I} by cellular reductants [such as NADH, ascorbic acid (AA), GSH, or the protein itself] to form stable species with features similar to those of copper complexes with Aβ peptides.[25] The $\alpha S-Cu^{I}$ complex can then catalyze the reduction of molecular oxygen O_2 into ROS, such as H_2O_2 and $OH^{\bullet}$ (eqs 1−4), which results in protein damage through oxidation of specific amino acid residues:

$$\alpha S-Cu^{2+} + e^{-} \rightarrow \alpha S-Cu^{+} \quad (1)$$

$$\alpha S-Cu^{+} + O_2 \rightarrow \alpha S-Cu^{2+} + O_2^{-} \quad (2)$$

$$2O_2^{-} + 2H^{+} \rightarrow O_2 + H_2O_2 \quad (3)$$

$$H_2O_2 + \alpha S-Cu^{+} \rightarrow OH^{-} + OH^{\bullet} + \alpha S-Cu^{2+} \quad (4)$$

$Cu^{II}-\alpha S$ binding has been extensively elucidated by using both full-length protein, point mutants,[22,27−36] and ad hoc designed model peptides.[37−41] All of the obtained findings suggest the N-terminus and His-50 as Cu^{II} donor residues. On the contrary, very few reports describing the nature of $Cu^{I}-\alpha S$ binding sites are available.[27,42] αS contains two regions, αS_{1-5} and $\alpha S_{116-127}$, located at the N and C termini, respectively, containing two Met residues and arranged as $[M(X)_nM]$, motifs which are commonly found in other proteins involved in copper homeostasis.[43−48] NMR investigations of full-length αS and its derived fragment, αS_{1-6}, have revealed that the main Cu^{I} anchoring site involves Met-1 and Met-5 sulfur-donor atoms,[42] whereas the C-terminal site was proposed to be less effective in metal binding.[27]

In this study, we have investigated $\alpha S-Cu^{I}$ interaction by means of NMR and circular dichroism (CD) analysis on the full-length αS (αS_{1-140}) and on the fragments αS_{1-15} (^{1}MDVFMKGLSKAKEGV$^{15}-NH_2$) and $\alpha S_{113-130}$ (Ac-^{113}LEDMPVDPDNEAYEMPSE^{130}-NH_2), both containing the $[M(X)_nM]$ motif found at the N and C termini, respectively. In order to further identify and characterize the metal binding environment in full-length αS, besides Cu^{I}, we have also used Ag^{I} as a probe for Cu^{I} binding. In fact, Ag^{I}, being isoelectronic with Cu^{I}, is amenable to NMR studies and redox-inactive and may be commonly used to investigate Cu^{I} sites, as demonstrated by the structural similarity of complexes formed by Ag^{I} and Cu^{I}, including ligands with methionine-rich sites.[49−51] A comparison between the copper binding abilities of all of the investigated systems, together with an estimation of apparent K_d values at physiological pH, is discussed with the aim to getting helpful information on the bioinorganic chemistry of αS.

MATERIALS AND METHODS

Protein and Reagents. Human wild-type αS cDNA, amplified by polymerase chain reaction with synthetic oligonucleotides (Sigma-Aldrich) containing NcoI and XhoI restriction sites, was cloned into a pET-28a plasmid (Novagen, Merck KGaA, Darmstadt, Germany). Then the protein was expressed in *Escherichia coli* BL21 (DE3) cells. Overexpression of the proteins was achieved by growing cells in a LB medium or, for the ^{15}N-labeled protein, in a M9 minimal medium prepared with $^{15}NH_4Cl$ (Cambridge Isotope Laboratories, Inc., Andover, MA) at 37 °C until an appropriate optical density at 600 nm (OD600 nm) of 0.3−0.4, followed by induction with 0.1 mM isopropyl β-thiogalactopyranoside for 4−5 h. The cells were collected by centrifugation, and recombinant protein was recovered from the periplasm by osmotic shock, as previously described.[26] The periplasmic homogenate was then boiled for 15 min, and the soluble fraction, containing αS, was subjected to a two-step (35% and 55%) ammonium sulfate precipitation. The pellet was then resuspended, extensively dialyzed against 20 mM Tris-HCl (pH 8.0), loaded into a 6 mL Resource Q column (GE Healthcare, Fairfield, CT), and eluted with a 0−500 mM gradient of NaCl. Finally, the protein was dialyzed against water, lyophilized, and stored at −20 °C.

The N-terminal αS_{1-15} peptide was synthesized in a solid phase using Fmoc chemistry. A rink-amide resin was used as the solid support, so that the resulting peptides would be amidated at the C terminus. After removal of the peptide from the resin and deprotection, the crude product was purified by RP HPLC on a Phenomenex Jupiter Proteo C12 column, using a Jasco PU-1580 instrument with diode-array detection (Jasco MD-1510), with a semilinear gradient of 0.1% trifluoroacetic acid (TFA) in water to 0.1% TFA in CH_3CN over 40 min. The identity of the peptide was confirmed by electrospray ionization mass spectrometry (Thermo-Finnigan). The purified peptide was lyophilized and stored at −20 °C until use.

The C-terminal $\alpha S_{113-130}$ peptide was purchased from Biomatik.

NMR and CD Spectroscopic Measurements. Full-length αS protein was dissolved in a 20 mM phosphate buffer in water at pH 7.4, obtaining a final concentration of 240 μM for NMR experiments and 10 μM for CD experiments. The protein concentration was estimated by a spectrometer using a molar extinction coefficient at 274 nm of 5960 M^{-1} cm^{-1}.[52] Peptides were dissolved in a 20 mM phosphate buffer in water at pH 7.4, obtaining a final concentration ranging from 400 to 500 μM for NMR experiments and 100 μM for CD experiments. The desired concentration of Ag^{I} ions was achieved by using a stock solution of 20 mM $AgNO_3$ (Sigma Chemical Co.) in D_2O. For copper(I) complexes, a 10 mM $[Cu(CH_3CN)_4]BF_4$ stock solution was prepared in a 20 mM phosphate buffer in D_2O at pH 7.4 (containing 5% v/v CH_3CN). 1.0 mM AA was added to both full-length protein and peptides just before use in order to avoid any possible oxidation of Cu^{I} to Cu^{II}. All of the solutions were degassed with water-saturated N_2 just before use and kept under an inert N_2 atmosphere. 3-(Trimethylsilyl)-[2,2,3,3-d_4]propansulfonate, sodium salt, was used as the internal reference standard for NMR measurements.

CD spectra were acquired on a Jasco J-815 spectropolarimeter at 288 K. A 0.1 cm cell path length was used for data between 180 and 260 nm, with a 1 nm sampling interval. Four scans were collected for every sample with a scan speed of 100 nm min^{-1} and a bandwidth of 1 nm. Baseline spectra were subtracted from each spectrum, and data were smoothed with the Savitzky−Golay method.[53] Data were processed using an *Origin 5.0* spread sheet/graph package. The direct CD measurements (θ, in millidegrees) were converted to mean residue molar ellipticity, using the relationship mean residue $\Delta\varepsilon = \theta/(33000cl \times \text{number of residues})$, where c and l refer to the molar concentration and cell path length, respectively.

NMR spectra were acquired at 278 and 288 K using Bruker Advance spectrometers operating at proton frequencies of 600 and 900 MHz, with the last one equipped with a cryoprobe. NMR spectra were processed with *XwinNMR 3.6* and *TopSpin 2.0* software and analyzed with the program *Cara*.[54] Suppression of the residual water signal was achieved either by presaturation or by excitation sculpting,[55] using a selective 2-ms-long square pulse on water. The proton resonance assignment of the peptides was obtained by 2D $^{1}H-^{1}H$ COSY, TOCSY, and NOESY experiments. The metal-interaction studies were performed by acquiring 2D $^{1}H-^{15}N$ HSQC and $^{1}H-^{13}C$ HSQC and 3D ^{15}N NOESY HSQC.

Structure Determination. NOE cross peaks in 2D $^{1}H-^{1}H$ NOESY spectra acquired on $\alpha S_{1-15}-Ag^{I}$ and $\alpha S_{113-130}-Ag^{I}$ complexes at 278 K were integrated with the *Cara* program and were converted

dx.doi.org/10.1021/ic302050m | *Inorg. Chem.* 2013, 52, 1358−1367

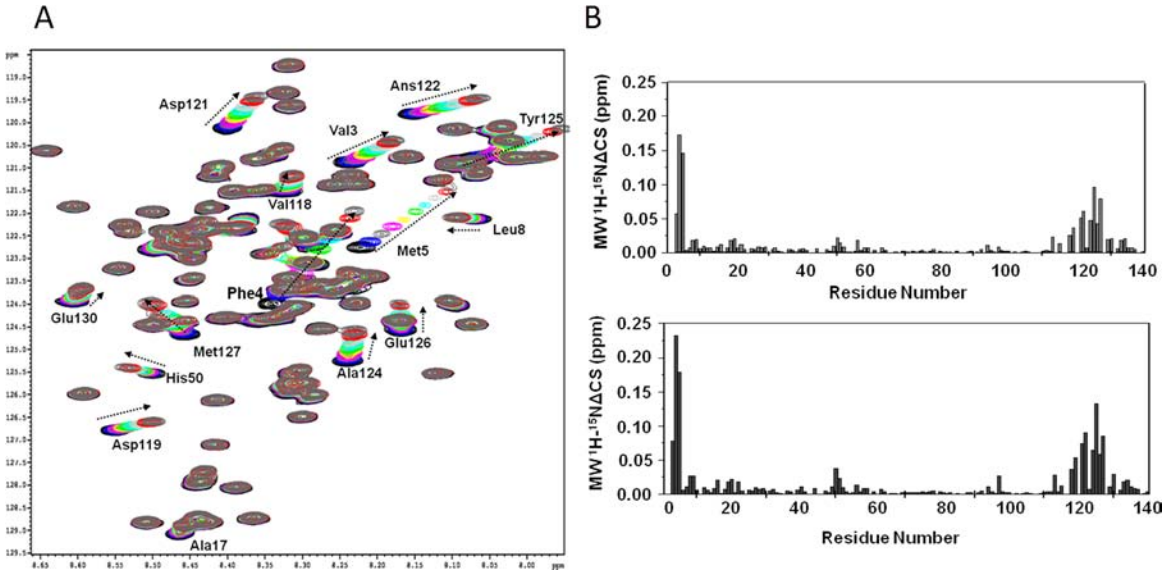

Figure 1. NMR analysis of Ag^I binding to full-length αS_{1-140}. (A) Overlaid $^1H-^{15}N$ HSQC spectra of αS_{1-140} in the presence of increasing amounts of Ag^I: 0 equiv (black), 0.125 equiv (blue), 0.250 equiv (gray), 0.375 equiv (magenta), 0.5 equiv (yellow), 0.65 equiv (green), 0.8 equiv (cyan), 1 equiv (light gray), 1.5 equiv (red), and 2 equiv (dark gray). (B and C) Differences in the mean weighted chemical shift displacements (MW $^1H-^{15}N$ ΔCS) between free and Ag^I-complexed αS_{1-140} at molar ratios of 1:1 (B) and 2:1 (C). The amide protons of Met-1 and Asp-2 were not detectable because of solvent exchange effects.

into upper internuclear distances with the routine *CALIBA* of the program package *DYANA*.[56] The intra- and interresidual constraints obtained were used to generate an ensemble of 30 structures by the standard protocol of simulated annealing in torsion angle space implemented in *DYANA* (using 10000 steps). To take into account the observed coordination behavior of silver, additional metal−proton distance constraints were imposed. No dihedral angle restraints and no hydrogen-bonding restraints were applied. The final structures were analyzed using the program *MOLMOL*.[57]

RESULTS

αS_{1-140}−Ag^I Interaction. The effects of Cu^I on NMR resonances of αS were first evaluated by comparing the $^1H-^{13}C$ HSQC spectrum of αS_{1-140} in the absence or in the presence of 0.5 equiv of Cu^I. Met-1, Met-5, Met-116, and Met-127 overlapping cross peaks assigned to Hε−Cε and Hγ−Cγ were the ones most affected by the presence of the metal ion (Figure 1S in the Supporting Information). To be sure that the effects we observed did not occur from oxidation of the αS−Cu^I to αS−Cu^{II} complex, the $^1H-^{13}C$ HSQC spectrum of αS_{1-140} in the presence of 0.5 equiv of Cu^{II} was recorded as well. No effects were observed for Hε−Cε and Hγ−Cγ cross peaks of Met-1, Met-5, Met-116, and Met-127. On the contrary, the addition of Ag^I to αS_{1-140} resulted in very similar $^1H-^{13}C$ HSQC spectra, supporting the suitability of Ag^I as a probe for Cu^I in the study of metal binding properties of αS. In fact, also in this case, the cross peaks assigned to Hε−Cε and Hγ−Cγ of Met-1, Met-5, Met-116. and Met-127 were the most affected ones (Figure 1S in the Supporting Information). All of these findings confirm that the thioether groups of Met are involved in the copper(I) coordination sphere[27,42] and indicate that silver ions have binding properties very similar to those of the cuprous ion.

More detailed information on the Ag^I binding regions in the full-length protein was obtained by recording $^1H-^{15}N$ HSQC spectra at 288 K on uniformly ^{15}N-enriched αS, gradually increasing the amount of metal, and monitoring the metal-induced changes in the spectra. The addition of the diamagnetic ion to the protein solutions at pH 7.4 caused selective shifts of both proton and nitrogen resonances of several residues (Figure 1). The largest effects were localized at both the N and C termini of the protein, with the major displacements observed for Val-3, Phe-4, Met-5, Asp-121, Asn-122, Tyr-125, and Met-127. His-50 and residues nearby (48−52) were affected as well, although to a lesser extent. However, no effects were observed on imidazolic protons of His-50 in 1D ^1H spectra (Figure 2S in the Supporting Information), suggesting that this residue, and therefore region 48−52, is not involved in Cu^I/Ag^I binding.

A 3D ^{15}N NOESY HSQC spectrum was also recorded, in order to establish if any interplay between the identified Ag^I binding motifs in the full-length protein occurs. No NOE interactions between the N- and C-terminal regions were identified, suggesting the occurrence of two separate, independent metal binding sites, encompassing 1−5 and 116−127 regions, respectively. On the other hand, we identified a contiguous series of intraresidual $H^N_i-H^N_{i+1}$ NOE interactions in the C-terminal 119−130 region. Because no residual structure has been identified in the free monomeric state of αS in water,[58] the appearance of NOE cross peaks in the C-terminal region of the protein is likely due to the binding of Ag^I, which induces structural rearrangements of that region.

These findings were also confirmed by far-UV CD spectroscopy. CD spectra were recorded on αS solutions and on solutions just containing $AgNO_3$ in order to exclude any interferences due to the use of nitrate salt. The spectra of both the free ligand and silver(I) complex showed a strong negative band at 198 nm (Figure 2), which is a diagnostic feature of random-coil conformations. However, the intensity of the random-coil band is progressively decreased as the metal concentration is increased (Figure 2), suggesting partial Ag^I-induced structuring of the main chain. The small extent of spectral modification confirms the unlikelihood of the occurrence of any interplay between the two different regions of the protein involved in Ag^I binding.

dx.doi.org/10.1021/ic302050m | *Inorg. Chem.* 2013, 52, 1358−1367

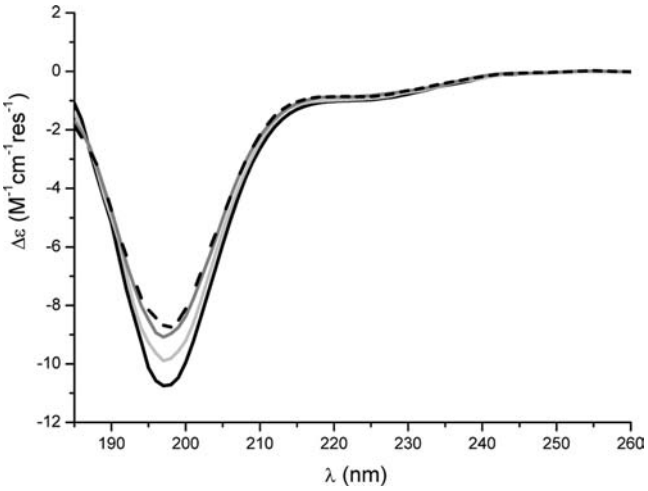

Figure 2. Far-UV CD spectra at 288 K of 10 μM full-length αS at pH 7.4. Spectra were recorded at different Ag^I concentrations: 0 equiv (black), 1 equiv (light gray), 2 equiv (dark gray), and 5 equiv (dashed black).

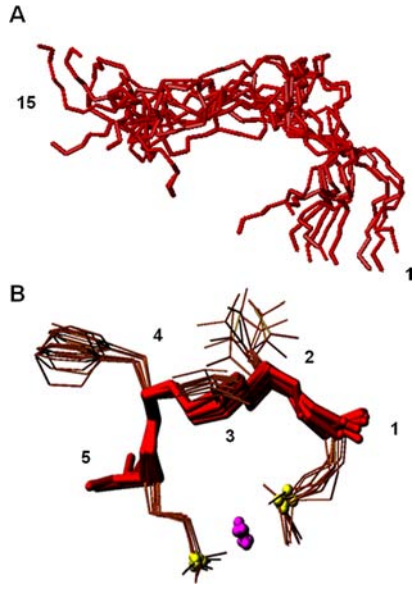

Figure 3. Superimposition of the first 10 structures obtained for the αS_{1-15}–Ag^I complex. The structures are fitted on all of the backbone residues (A) and on the 1–5 backbone residues (B). The sulfur-donor atoms of Met-1 and Met-5 are shown as yellow spheres. The silver ion is shown as a magenta sphere.

In order to obtain more detailed information on the specificity of the Ag^I binding to αS, we investigated the metal binding features of two synthetic peptides, αS_{1-15} and $\alpha S_{113-130}$, encompassing the two regions of the full-length protein that were significantly affected by the presence of the metal ion.

αS_{1-15}–Ag^I Complex. The details of Ag^I binding to αS_{1-15} were explored at single-residue resolution using 1D and 2D ^{1}H NMR spectroscopy.

The NMR investigation was performed on 400 μM peptide samples at pH 7.4 in a 20 mM phosphate buffer at 288 K. The addition of silver ion to the peptide solution caused selective proton chemical shift displacements similar to those observed for the Cu^I–αS_{1-6} system[42] (Figure 3S in the Supporting Information). The largest effects were observed for Met-1 and Met-5 and residues nearby (Val-3, Phe-4, and Met-5), confirming the involvement of Met thioether groups in the metal binding.[42] On the contrary, no chemical shift displacements were detected for residues 7–15, indicating that these protons are distant from the metal binding site. Further analysis of ^{1}H–^{13}C HSQC spectra showed substantial ^{13}C and ^{1}H downfield shifting of both Met-1 and Met-5 ε-CH_3, γ-CH_2, and β-CH_2 groups and smaller effects on Met-1 Cα–Hα, Asp-2 Cα–Hα and Cβ–Hβ, Val-3 Cα–Hα, Cβ–Hβ, and Cγ–Hγ, and Phe-4 Cβ–Hβ cross peaks (Figure 4S in the Supporting Information). These findings strongly support Met-1 and Met-5 residues as the silver binding region with the Met δ-sulfur atoms bound to Ag^I and confirm that previously found for Cu^I–αS_{1-6} systems.[42]

This information, together with the ^{1}H–^{1}H distances obtained from the NOESY spectrum recorded at 278 K, was successively employed as restraints for the structure determination of the αS_{1-15}–Ag^I complex, by using the *DYANA* program (see the experimental section for details). The obtained first 10 structures are shown in Figure 3. When fitted on all of the backbone residues, the absence of any preferred conformation is easily observed (Figure 3A), as confirmed by the high values of root-mean-square deviation (RMSD) for the backbone and heavy atoms, respectively 3.54 ± 1.05 and 4.89 ± 1.30 Å. On the contrary, following the fitting on the silver binding domain, 1–5 residues (Figure 3B), the structures assume a well-defined arrangement and the calculated RMSD values are 0.39 ± 0.18 and 1.03 ± 0.26 Å, respectively, for the backbone and heavy atoms.

The absence of any preferred secondary structure is confirmed also by CD spectra (Figure 5S in the Supporting Information). Both the free ligand and silver(I) complex showed the intense negative band at 198 nm representative of random-coil conformation.[59] Increasing the amount of metal did not further affect the spectrum.

$\alpha S_{113-130}$–Ag^I Complex. Ag^I binding to the $\alpha S_{113-130}$ fragment was explored by means of 1D and 2D ^{1}H NMR and CD spectroscopy.

NMR spectra were recorded at 288 K on 400 μM peptide samples at pH 7.4 in a 20 mM phosphate buffer. The addition of Ag^I to the peptide solution caused selective proton chemical shift displacements in ^{1}H–^{1}H TOCSY spectra. The most affected amide protons belong to Asn-122 and Tyr-125 (Figure 4A). Amide protons of Met-116, Met-127, Asp-115, Asp-121, and Glu-123 were affected as well, although to a lesser extent. However, analysis of the aliphatic region (Figure 4B) showed that the major displacements occur for Hβ and Hγ protons of Met-116 and Met-127, indicating their proximity to the metal ion, while only small chemical shift variations were observed for the side-chain protons of Val-118, Asp-119, Asn-122, and Tyr-125.

^{1}H–^{13}C HSQC spectra were additionally recorded to evaluate the effect of silver binding to $\alpha S_{113-130}$. Among all of the observed resonances, the Cε–Hε cross peaks assigned to Met-116 and Met-127 exhibited the most significant chemical shift variations (Figure 6S in the Supporting Information). Cross peaks assigned to Cγ–Hγ and Cβ–Hβ of methionine residues were shifted as well, whereas no changes were observed on signals belonging to the other residues of the sequence, except for Cβ–Hβ cross peaks assigned to proline residues, likely because of the structural rearrangement of the peptide backbone. All of the collected findings strongly indicate the δ-sulfur atoms of Met-116 and Met-127 side chains as the silver binding donors.

dx.doi.org/10.1021/ic302050m | *Inorg. Chem.* 2013, 52, 1358–1367

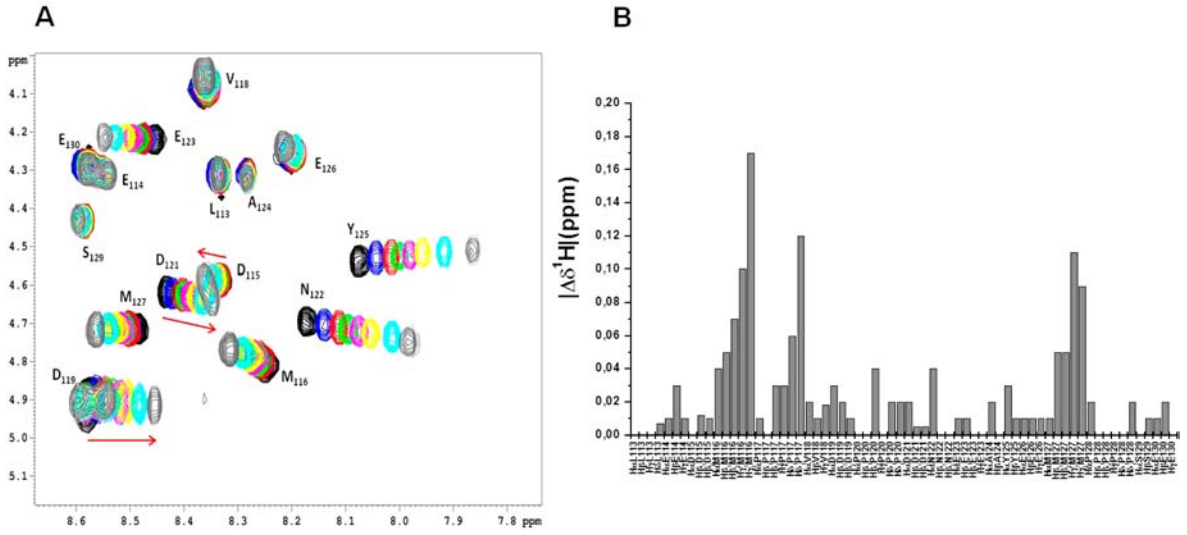

Figure 4. (A) Overlaid ^{1}H−^{1}H TOCSY spectra amide region of $\alpha S_{113-130}$ in the presence of increasing amounts of $AgNO_3$: 0 equiv (black), 0.125 equiv (blue), 0.2 equiv (red), 0.3 equiv (green), 0.6 equiv (magenta), 0.8 equiv (yellow), 1 equiv (cyan), 1.5 equiv (light gray), and 3 equiv (dark gray). (B) Chemical shift displacements of the aliphatic region of ^{1}H−^{1}H TOCSY spectra recorded in the absence and presence of 1 equiv of Ag^I.

^{1}H−^{1}H NOESY experiments at 278 K were performed on the $\alpha S_{113-130}$−Ag^I complex in order to obtain structural information. The spectrum obtained in the presence of 1 equiv of $AgNO_3$ showed several dipolar correlations, which were converted into a set of distance constraints. Interestingly, the spectrum showed the occurrence of interresidual H^N_i−H^N_{i+1} NOE interactions in the region encompassing residues 121−126 (Figure 5), resembling the behavior observed for the

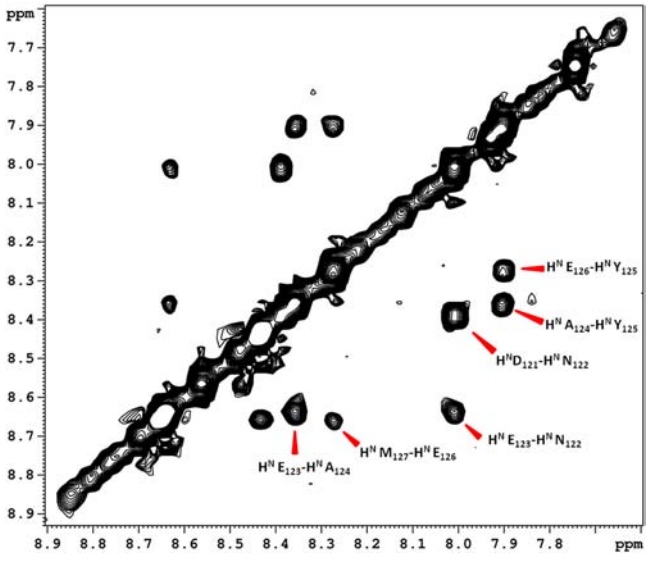

Figure 5. ^{1}H−^{1}H NOESY spectrum of 400 μM $aS_{113-130}$ recorded in the presence of 1 equiv of $AgNO_3$ at 278 K and pH 7.4.

full-length protein. This observation can also explain the large chemical shift variation observed for the amide protons of these residues. The distance values obtained from NOESY, together with the binding distances between the silver ion and Met-116 and Met-127 δ-sulfur atoms, were used as constraints for determining the structure of the metal complex, by using the *DYANA* program. The first 10 structures obtained are reported in Figure 6, which shows the occurrence of a bent backbone in the region encompassing the two methionine residues and the metal ion.

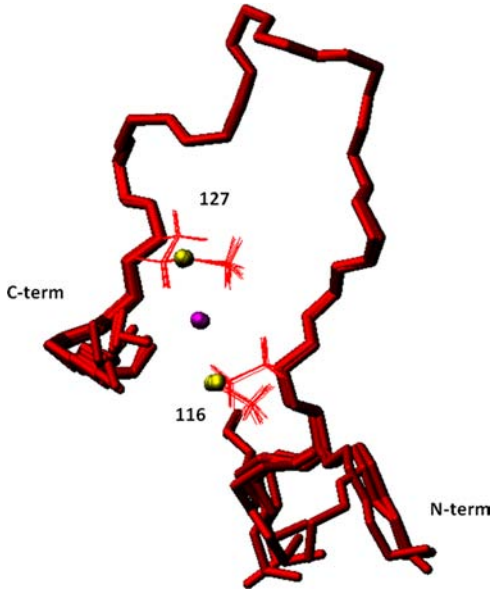

Figure 6. Superimposition of the first 10 structures obtained for the $\alpha S_{113-130}$−Ag^I complex. The structures are fitted on 116−127 backbone residues. The sulfur-donor atoms of Met-116 and Met-127 are shown as yellow spheres. The silver ion is shown as a magenta sphere.

Far-UV CD spectroscopy confirmed the results obtained with NMR. The spectrum of the free $\alpha S_{113-130}$ at 288 K is characteristic of a random-coil peptide, showing a strong negative band at 198 nm (Figure 7S in the Supporting Information). Upon Ag^I addition, the intensity of the random-coil band is reduced and a weak negative band at 220 nm appears.

Finally, we monitored the interaction of $\alpha S_{113-130}$ with Cu^I in order to directly compare the Ag^I and Cu^I behaviors. ^{1}H−^{1}H TOCSY and ^{1}H−^{13}C HSQC spectra of $\alpha S_{113-130}$ in the presence of 1 equiv of Cu^I showed very similar chemical shift

dx.doi.org/10.1021/ic302050m | *Inorg. Chem.* 2013, 52, 1358−1367

displacements (Figure 7), suggesting the occurrence of similar metal−peptide interactions. The $^{1}H-^{13}C$ HSQC spectrum

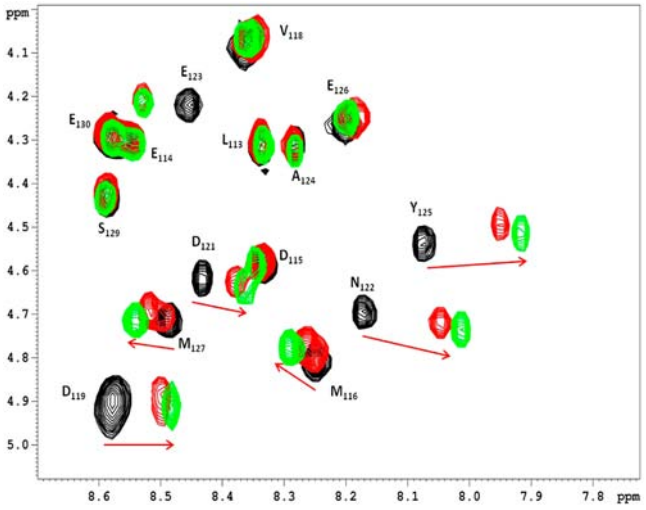

Figure 7. Overlaid $^{1}H-^{1}H$ TOCSY spectra amide proton region of $\alpha S_{113-130}$ in the absence (black) and presence of 1 equiv of Cu^{I} (red) and 1 equiv of Ag^{I} (green).

suggested, as in the case of Ag^{I}, the binding of Cu^{I} to the δ-sulfur atom on the methionine residue side chain, with the cross peaks assigned to ε-CH_3 groups of Met-116 and Met-127 being the most shifted, together with β- and γ-CH_2 methionine group cross peaks (data not shown).

Comparison of the Binding Affinities. In order to evaluate and compare the binding affinity of Cu^{I}/Ag^{I} sites in αS_{1-15} and $\alpha S_{113-130}$, we additionally investigated silver coordination to a binary system containing both peptides. The fingerprint regions of $^{1}H-^{1}H$ TOCSY spectra of such a solution were compared with the corresponding ones of αS_{1-15} or $\alpha S_{113-130}$ in both the presence and absence of Ag^{I}. Figure 8A shows that the NH−Hα correlations of the two apo αS_{1-15} and $\alpha S_{113-130}$ peptides (displayed in green and magenta, respectively) are well superimposed on the corresponding ones in the binary system (black contours), indicating that no interaction between peptides occurs under these conditions. Furthermore, we found that the addition of 1.0 equiv of Ag^{I} to solutions containing both αS_{1-15} and $\alpha S_{113-130}$ (black contours, Figure 8B) resulted in chemical shift variations very similar to those detected for each single peptide in the presence of 0.5 equiv of Ag^{I} (green and magenta contours for αS_{1-15} and $\alpha S_{113-130}$, respectively). Such data indicate that αS_{1-15} and $\alpha S_{113-130}$ possess very similar binding affinities and suggest that Ag^{I} ions are equally distributed among the two binding sites. In fact, as shown in Figure 8C, further addition of silver to the binary system (1.6 equiv of Ag^{I}) resulted in effects almost identical with the ones detected for αS_{1-15} and $\alpha S_{113-130}$ with 0.8 equiv of Ag^{I}. Finally, we compared the NH chemical shift variations detected for the binary solution with those found for the same residues in the full-length protein (Figure 9). Nicely, the recorded effects are very similar, strongly supporting the indication that the two binding sites might compete for copper/silver binding in the full-length αS as well.

The apparent K_d constant of silver association at both binding sites was further evaluated by analysis of NMR and CD spectra, obtained upon titrations of both αS_{1-15} and $\alpha S_{113-130}$ fragments with Ag^{I}. Chemical shift variations of selected proton resonances in the amide region of the $^{1}H-^{1}H$ TOCSY spectra recorded with increasing concentrations of metal ion were measured and used to build affinity binding curves for the three systems. For αS_{1-15} and $\alpha S_{113-130}$ fragments, data were fit to a model incorporating one Ag^{I} ion per molecule (with dissociation constant K_d) by using the program *DynaFit*.[60] Changes in the chemical shift values of amide resonances of Val-3, Phe-4, and Met-5 were used to evaluate the affinity toward Ag^{I} of the N-terminal binding site αS_{1-15}, whereas Met-116 and Met-127 amide resonances were used to evaluate the affinity of $\alpha S_{113-130}$ toward the Ag^{I} ion (Figure 8S in the Supporting Information). The obtained results gave an apparent K_d value in the micromolar range and confirmed the 1:1 stoichiometry for both fragments, further supporting similar binding affinities.

DISCUSSION

The interaction of αS with metal ions, and in particular with copper, is widely considered to play a critical role in the etiology of PD.

Cu^{II} binding to αS has been shown either to induce aggregation and precipitation of αS or to catalyze the production of H_2O_2 and other ROS, which are involved in oxidative stress and resulting in damage and loss of dopaminergic cells in PD brain.

Recently, it has been shown that the redox potential of $\alpha S-Cu^{II}/\alpha S-Cu^{I}$ (0.018 V vs Ag/AgCl) is higher than that of various highly abundant cellular reductants such as AA, NADH, GSH, etc.;[24] therefore redox reactions involving a $\alpha S-Cu^{II}/\alpha S-Cu^{I}$ couple are likely to occur, and these may be responsible for the depletion of GSH in the *substantia nigra* of PD patients, considered to be strong evidence of the oxidative stress hypothesis.[1,61] Moreover, it has been demonstrated that, even though a $\alpha S-Cu^{II}/\alpha S-Cu^{I}$ redox pair cannot directly oxidize dopamine, it can generate H_2O_2 (as described in eqs 1 and 2), which, on the contrary, does.[61,62]

In order to enhance understanding of the role, if any, played by αS in oxidative stress, it is essential to characterize first the Cu^{I}/Cu^{II} binding mode to αS. So far, the majority of the studies have focused on the investigation of Cu^{II} interaction with αS. Two metal binding sites have been identified and well characterized: one at the N termini of the protein and the second one centered at His-50 (see ref 27 for a review). On the contrary, very few investigations have been carried out on the interaction of αS with Cu^{I}. Recently, Cu^{I} binding to full-length αS at pH 6.5 was investigated by Binolfi and co-workers.[42] The study has identified and characterized one Cu^{I} binding site located at the N-terminal region of the protein, with the δ-sulfur atoms of Met-1 and Met-5 indicated as the Cu^{I} donor group. The NMR-derived dissociation constant K_d is in the micromolar range, in full agreement with values from previous reports on Cu^{II} binding to proteins and peptides involving Met residues as primary metal-anchoring ligands.[63,64] Moreover, such association values indicate the existence of a finite probability to have Cu^{I} bound to αS. The formed complex, also at very low concentration, might have catalytic activity, amplifying the toxic effects associated with ROS formation.

In this work, NMR and CD spectroscopies were used in order to characterize all of the possible Cu^{I} binding regions in αS. In addition to Cu^{I}, we have used Ag^{I} as a probe for Cu^{I} binding to the protein. Ag^{I} is a diamagnetic, NMR-active metal ion, and it is therefore amenable to NMR studies. Because it is redox-inactive, Ag^{I} is often used to investigate Cu^{I} sites. The

dx.doi.org/10.1021/ic302050m | *Inorg. Chem.* 2013, 52, 1358−1367

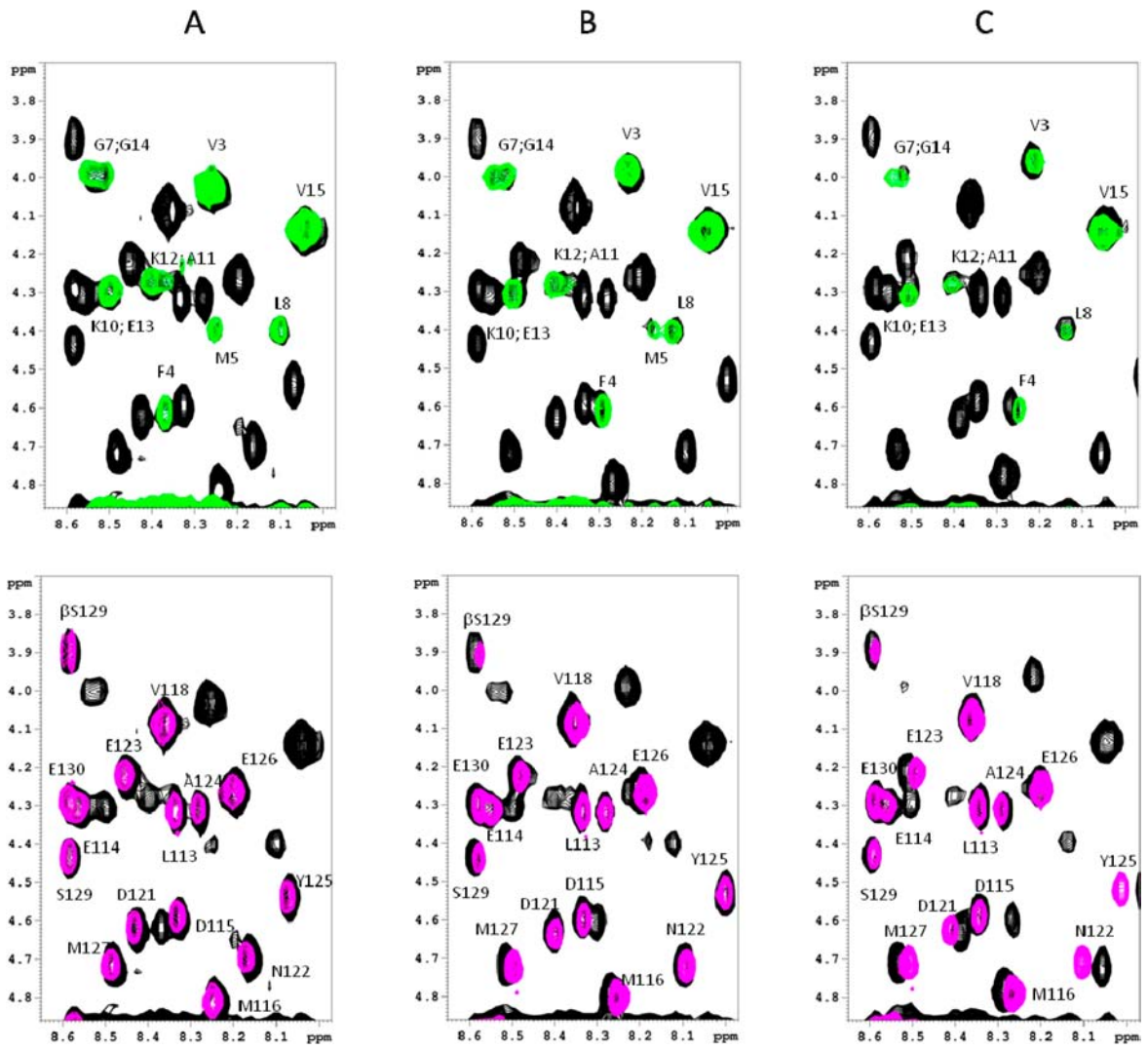

Figure 8. Overlaid $^{1}H-^{1}H$ TOCSY fingerprint regions of a $\alpha S_{1-15}-\alpha S_{113-130}$ binary system (black) and of αS_{1-15} (green) or $\alpha S_{113-130}$ (magenta): (A) apo solution; (B and C) different Ag^{I} addition. For a $\alpha S_{1-15}-\alpha S_{113-130}$ binary system (black countours), additions of 1.0 and 1.6 equiv of Ag^{I} are shown in parts B and C, respectively. For αS_{1-15} (green countours) or $\alpha S_{113-130}$ (magenta countours), additions of 0.5 and 0.8 equiv of Ag^{I} are shown in parts B and C, respectively.

two ions have, in fact, identical d-shell electron configurations (d^{10}) and oxidation states, and although Ag^{I} is larger than Cu^{I}, in many cases it adopts complexes similar to those formed by Cu^{I}. The fact that, unlike Cu^{I}, silver it is not susceptible to oxidation has led to its use as a probe of Cu^{I} sites in proteins such as metallothionein, in which it displays a high affinity for cysteine-rich sites[65−67] or in methionine-rich sites.[49]

The chemical shift variations of amide groups recorded for the full-length αS protein (Figure 1) after the addition of Ag^{I} are very similar to the ones previously measured for Cu^{I},[42] strongly indicating analogue coordination environments for both metal ions. Furthermore, the effects detected on αS_{1-15} upon Ag^{I} addition (Figures 3S and 4S in the Supporting Information) were comparable to the ones reported for the $\alpha S_{1-6}-Cu^{I}$ complex, where the Met-1 and Met-5 thioether groups coordinate to Cu^{I}.[42]

The absence of significant conformational changes of αS upon Ag^{I} binding, shown by invariance of the far-UV CD spectra (Figure 2), together with the absence of any NOE interaction between the N- and C-terminal regions of αS, suggests the unlikelihood of any interplay between the two sites in metal binding such as to allow the use of two model peptides, each containing a single metal binding site, for characterization of the metal coordination sphere at the molecular level. A series of 1D and 2D homo- and heteronuclear experiments recorded in the presence of increasing amounts of metal revealed a 1:1 stoichiometry for Ag^{I}/Cu^{I} binding to both the N-terminal (αS_{1-15}) and C-terminal ($\alpha S_{113-130}$) fragments. The effects observed for the two fragments were fully in agreement with those observed for the full-length protein, supporting the suitability of the two peptides as models for copper/silver binding sites in αS (Figure 9). A very similar silver/copper binding mode was detected for the two sites. In both cases, coordination of Ag^{I} by δ-sulfur atoms of methionine residues was widely supported by the changes detected in the NMR spectra, with the major chemical shift variations observed for methionine amide and side-chain protons. The significant H^{N} chemical shift modifications detected for Val-3 and Phe-4 at the N terminus or Asn-122 and Tyr-125 at the C terminus were attributed to the sensitivity of amide protons to very local effects, such as backbone torsion angle modification, steric clash occurrence, etc., rather than to

dx.doi.org/10.1021/ic302050m | Inorg. Chem. 2013, 52, 1358−1367

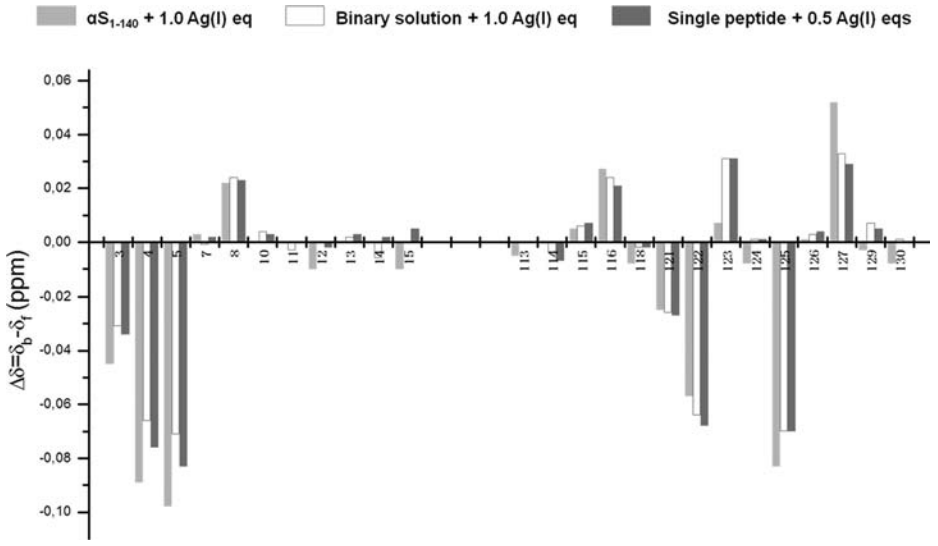

Figure 9. Chemical shift variations of amide protons due to Ag^I binding in the full-length protein (light gray) in the αS_{1-15}–$\alpha S_{113-130}$ binary system (white) and in αS_{1-15} and $\alpha S_{113-130}$ fragments (gray).

electronic effects due to metal coordination. The absence of chemical shift variations of the side-chain protons of these residues likely confirms our assumption. In particular, for the N-terminal binding site, the participation of Met-1 NH_2 group in copper coordination was hypothesized,[27] but the same chemical shift variation experienced by both Met-1 and Met-5 Hα (Figure 3S in the Supporting Information) allows us to exclude this possibility. Furthermore, the obtained 3D NMR structure of the Ag^I–αS_{1-15} and Ag^I–$\alpha S_{113-130}$ complexes (Figures 3 and 6) supported interaction of the Ag^I ion with the sole methionine sulfur atoms because no other side chains are found in the proximity of the metal ion in any of the 30 structures generated.

Even though in both sites Cu^I and Ag^I experience the same coordination environment, more detailed NMR and CD analysis of the single fragments pointed out some differences in terms of metal-induced conformational effects. On the one hand, no changes in the native random-coil backbone conformation are visible for the N-terminal fragment, as shown either by the similarity between the CD spectra recorded on both the apo-αS_{1-15} and the Ag^I–αS_{1-15} complex (Figure 5S in the Supporting Information) or by the absence of any nontrivial NOEs in the ^1H–^1H NOESY spectrum, which result in a 3D structure with no preferred conformations. On the other hand, the C-terminal $\alpha S_{113-130}$ site undergoes large structural modification upon Ag^I binding. Both CD and NOESY spectra clearly show modification of the backbone conformation, with a decrease of the random-coil content (Figure 7S in the Supporting Information) and the appearance of sequential interresidual H^N_i–H^N_{i+1} NOEs in the region encompassing residues 121–127 (Figure 5). The obtained 3D NMR structure confirmed the occurrence of a bent backbone, stabilized by the formation of a hydrogen bond between Ala-124 H^N and Asp-121 CO and between Met-127 H^N and Asp-123 CO, typically found in β-turn conformations, observed in almost all of the 30 generated structures. Nicely, the NOE patterns observed for the C-terminal complex resemble the ones observed for the full-length αS_{1-140}, where interresidual H^N_i–H^N_{i+1} NOEs appear as well, although in a more extended region (encompassing residues 118–130).

Besides the different structural effects induced by Ag^I binding to the N- and C-terminal fragments, competition studies carried out on ternary systems containing both N- and C-terminal fragments and Ag^I showed that the metal binds to both sites with very similar affinities. The NMR- and CD-based estimation of the dissociation constants gave apparent K_d values in the 10^{-5}–10^{-6} M range for both silver binding sites. Moreover, a comparison between the effects recorded on the ternary system and the ones recorded on the full-length αS showed very similar proton chemical shift displacements (Figure 9), supporting the hypothesis that the two binding sites may compete for copper/silver binding. Finally, the two metal binding domains, located far away from the NAC region involved in protein fibrilization, are consistent with similar copper binding behaviors in fibrils, which might indeed have redox activity similar to that of the monomer system.

CONCLUSIONS

In this work, the structural details of Cu^I/Ag^I binding to αS were investigated by CD and NMR spectroscopy. A comparison between the metal-induced effects monitored on the full-length protein and on two *ad hoc* designed model peptides indicated the existence of two separate Cu^I/Ag^I binding domains encompassing the 1–5 and 116–127 regions, respectively. Both domains exhibit similar metal binding affinities and comparable metal coordination spheres, characterized by two Met sulfur atoms likely in a linear geometry, as shown in previously investigated two-coordinated copper(I) model complexes.[68] However, further investigations would be necessary to determine the exact metal geometry. NMR structural characterization of the two binding sites showed that metal interaction at the N termini does not yield any particular structural rearrangements; on the contrary, the binding to Met-116 and Met-127 induces a β-turn backbone conformation stabilized by Ala-124 H^N–Asp-121 CO and Met-127 H^N–Asp-123 CO hydrogen bonds.

dx.doi.org/10.1021/ic302050m | *Inorg. Chem.* 2013, 52, 1358–1367

■ ASSOCIATED CONTENT

Supporting Information

NMR and CD spectra, chemical shift variations, binding curves. This material is available free of charge via the Internet at http://pubs.acs.org.

■ AUTHOR INFORMATION

Corresponding Author

*E-mail: daniela.valensin@unisi.it.

Notes

The authors declare no competing financial interest.

■ ACKNOWLEDGMENTS

We thank MIUR (PRIN), CIRMMP (Consorzio Interuniversitario Risonanze Magnetiche di Metalloproteine Paramagnetiche), and CIRCMSB (Consorzio Interuniversitario di Ricerca in Chimica dei Metalli nei Sistemi Biologici) for financial support. The 900 MHz $^{1}H-^{15}N$ HSQC and 3D ^{15}N NOESY HSQC spectra were recorded at the CERM (Florence, Italy), which is kindly acknowledged.

■ REFERENCES

(1) Jenner, P. *Ann. Neurol.* **2003**, *53*, S26−S36.
(2) Ebadi, M.; Srinivasan, S. K.; Baxi, M. D. *Prog. Neurobiol.* **1996**, *48*, 1−19.
(3) Eriksen, J.; Dawson, T.; Dickson, D.; Petrucelli, L. *Neuron* **2003**, *40*, 453−456.
(4) Gasser, T. *J. Neurol.* **2001**, *248*, 833−840.
(5) Spillantini, M. G.; Schmidt, M. L.; Lee, V. M. Y.; Trojanowski, J. Q.; Jakes, R.; Goedert, M. *Nature* **1997**, *338*, 839−840.
(6) Uversky, V. N.; Oldfield, C. J.; Dunker, A. K. *Annu. Rev. Biophys.* **2008**, *37*, 215−246.
(7) Bertoncini, C. W.; Jung, Y. S.; Fernandez, C. O.; Hoyer, W.; Griesinger, C.; Jovin, T. M.; Zweckstetter, M. *Proc. Natl. Acad. Sci. U.S.A.* **2005**, *102*, 1430−1435.
(8) Jao, C. C.; Hegde, B. G.; Chen, J.; Haworth, I. S.; Langen, R. *Proc. Natl. Acad. Sci. U.S.A.* **2008**, *105*, 19666−19671.
(9) Ulmer, T. S.; Bax, A. *J. Biol. Chem.* **2005**, *280*, 43179−43187.
(10) Varadarajan, S.; Yatin, S.; Aksenova, M.; Butterfield, D. A. *J. Struct. Biol.* **2000**, *130*, 184−208.
(11) Zhu, M.; Qin, Z. J.; Hu, D.; Munishkina, L. A.; Fink, A. L. *Biochemistry* **2006**, *45*, 8135−42.
(12) Halliwell, B. *J. Neurochem.* **1992**, *59*, 1609−1623.
(13) Allsop, D.; Mayes, J.; Moore, S.; Masad, A.; Tabner, B. J. *Biochem. Soc. Trans.* **2008**, *36*, 1293−1298.
(14) Lovell, M. A. *J. Alzheimer's Dis.* **2009**, *16*, 471−483.
(15) Bolognin, S.; Messori, L.; Zatta, P. *Neuromol. Med.* **2009**, *11*, 223−238.
(16) Paik, S. R.; Shin, H. J.; Lee, J. H. *Arch. Biochem. Biophys.* **2000**, *378*, 269−277.
(17) Cole, S. H.; Carney, G. E.; McClung, C. A.; Willard, S. S.; Taylor, B. J.; Hirsh, J. *J. Biol. Chem.* **2005**, *280*, 14948−14955.
(18) Peña, M. M. O.; Lee, J.; Thiele, D. J. *J. Nutr.* **1999**, *129*, 1251−1260.
(19) Macomber, L.; Imlay, J. A. *Proc. Natl. Acad. Sci. U.S.A.* **2009**, *106*, 8344−8349.
(20) Bush, A. I. *Trends Neurosci.* **2003**, *26*, 207−214.
(21) Lucas, H. R.; Debeer, S.; Hong, M. S.; Lee, J. C. *J. Am. Chem. Soc.* **2010**, *132*, 6636−6637.
(22) Lucas, H. R.; Lee, J. C. *J. Inorg. Biochem.* **2010**, *104*, 245−249.
(23) Davies, P.; Wang, X.; Sarell, C. J.; Drewett, A.; Marken, F.; Viles, J. H.; Brown, D. R. *Biochemistry* **2011**, *50*, 37−47.
(24) Wang, C.; Liu, L.; Zhang, L.; Peng, Y.; Zhou, F. *Biochemistry* **2010**, *49*, 8134−8142.
(25) Jiang, D.; Men, L.; Wang, J.; Zhang, Y.; Chickenyen, S.; Wang, Y.; Zhou, F. *Biochemistry* **2007**, *46*, 9270−9282.
(26) Huang, C.; Ren, G.; Zhou, H.; Wang, C. *Protein Expression Purif.* **2005**, *42*, 173−177.
(27) Binolfi, A.; Quintanar, L.; Bertoncini, C. W.; Griesinger, C.; Fernandez, C. O. *Coord. Chem. Rev.* **2012**, *256*, 2188−2201.
(28) Kozlowski, H.; Luczkowski, M.; Remelli, M.; Valensin, D. *Coord. Chem. Rev.* **2012**, *256*, 2129−2141.
(29) Binolfi, A.; Rasia, R. M.; Bertoncini, C. W.; Ceolin, M.; Zweckstetter, M.; Griesinger, C.; Jovin, T. M.; Fernandez, C. O. *J. Am. Chem. Soc.* **2006**, *128*, 9893−9901.
(30) Binolfi, A.; Lamberto, G. R.; Duran, R.; Quintanar, L.; Bertoncini, C. W.; Souza, J. M.; Cervenansky, C.; Zweckstetter, M.; Griesinger, C.; Fernandez, C. O. *J. Am. Chem. Soc.* **2008**, *130*, 11801−11812.
(31) Binolfi, A.; Rodriguez, E. E.; Valensin, D.; D'Amelio, N.; Ippoliti, E.; Obal, G.; Duran, R.; Magistrato, A.; Pritsch, O.; Zweckstetter, M.; Valensin, G.; Carloni, P.; Quintanar, L.; Griesinger, C.; Fernandez, C. O. *Inorg. Chem.* **2010**, *49*, 10668−10679.
(32) Bortolus, M.; Bisaglia, M.; Zoleo, A.; Fittipaldi, M.; Benfatto, M.; Bubacco, L.; Maniero, A. L. *J. Am. Chem. Soc.* **2010**, *132*, 18057−18066.
(33) Lee, J. C.; Gray, H. B.; Winkler, J. R. *J. Am. Chem. Soc.* **2008**, *130*, 6898−6899.
(34) Jackson, M. S.; Lee, J. C. *Inorg. Chem.* **2009**, *48*, 9303−9307.
(35) Drew, S. C.; Leong, S. L.; Pham, C. L.; Tew, D. J.; Masters, C. L.; Miles, L. A.; Cappai, R.; Barnham, K. J. *J. Am. Chem. Soc.* **2008**, *130*, 7766−7773.
(36) Dudzik, C. G.; Walter, E. D.; Millhauser, G. L. *Biochemistry* **2011**, *50*, 1771−1777.
(37) Migliorini, C.; Porciatti, E.; Luczkowski, M.; Valensin, D. *Coord. Chem. Rev.* **2012**, *256*, 352−368.
(38) Ahmad, A.; Burns, C. S.; Fink, A. L.; Uversky, V. N. *J. Biomol. Struct. Dyn.* **2012**, *29*, 825−842.
(39) Drew, S. C.; Tew, D. J.; Masters, C. L.; Cappai, R.; Barnham, K. *J. Appl. Magn. Reson.* **2009**, *36*, 223−229.
(40) Kowalik-Jankowska, T.; Rajewska, A.; Jankowska, E.; Grzonka, Z. *Dalton Trans.* **2006**, *42*, 5068−5076.
(41) Valensin, D.; Camponeschi, F.; Luczkowski, M.; Baratto, M. C.; Remelli, M.; Valensin, G.; Kozlowski, H. *Metallomics* **2011**, *3*, 292−302.
(42) Binolfi, A.; Valiente-Gabioud, A. A.; Duran, R.; Zweckstetter, M.; Griesinger, C.; Fernandez, C. O. *J. Am. Chem. Soc.* **2011**, *133*, 194−196.
(43) Lee, J.; Peña, M. M.; Nose, Y.; Thiele, D. J. *J. Biol. Chem.* **2002**, *277*, 4380−4387.
(44) Puig, S.; Lee, J.; Lau, M.; Thiele, D. J. *J. Biol. Chem.* **2002**, *277*, 26021−26030.
(45) Cha, J. S.; Cooksey, D. A. *Proc. Natl. Acad. Sci. U.S.A.* **1991**, *88*, 8915−8919.
(46) Arnesano, F.; Banci, L.; Bertini, I.; Mangani, S.; Thompsett, A. R. *Proc. Natl. Acad. Sci. U.S.A.* **2003**, *100*, 3814−3819.
(47) Koay, M.; Zhang, L.; Yang, B.; Maher, M. J.; Xiao, Z.; Wedd, A. G. *Inorg. Chem.* **2005**, *44*, 5203−5205.
(48) Loftin, I. R.; Franke, S.; Roberts, S. A.; Weichsel, A.; Héroux, A.; Montfort, W. R.; Rensing, C.; McEvoy, M. M. *Biochemistry* **2005**, *44*, 10533−10540.
(49) Kihlken, M. A.; Singleton, C.; Le Brun, N. E. *J. Biol. Inorg. Chem.* **2008**, *13*, 1011−1023.
(50) Wimmer, R.; Herrmann, T.; Solioz, M.; Wuthrich, K. *J. Biol. Chem.* **1999**, *274*, 22597−22603.
(51) Loftin, I. R.; Franke, S.; Blackburn, N. J.; McEvoy, M. M. *Protein Sci.* **2007**, *16*, 2287−2293.
(52) Weinreb, P. H.; Zhen, W.; Poon, A. W.; Conway, K. A.; Lansbury, P. T., Jr. *Biochemistry* **1996**, *35*, 13709−13715.
(53) Savitzky, A.; Golay, M. J. E. *Anal. Chem.* **1964**, *36*, 1627−1639.
(54) Keller, R.; Wüthrich, K. *A New Software for the Analysis of Protein NMR Spectra*, 2002.
(55) Hwang, T. L.; Shaka, A. J. *J. Magn. Reson., Ser. A* **1995**, *112*, 275−279.

(56) Güntert, P.; Mumenthaler, C.; Wüthrich, K. *J. Mol. Biol.* **1997**, *273*, 283−298.
(57) Koradi, R.; Billeter, M.; Wüthrich, K. *J. Mol. Graph.* **1996**, *14*, 51−55.
(58) Eliezer, D.; Kutluay, E.; Bussell, R., Jr.; Browne, G. *J. Mol. Biol.* **2001**, *307*, 1061−1073.
(59) Greenfield, N. J.; Fasman, G. D. *Biochemistry* **1969**, *8*, 4108−4116.
(60) Kuzmic, P. *Anal. Biochem.* **1996**, *237*, 260−273.
(61) Sian, J.; Dexter, D. T.; Lees, A. J.; Daniel, S.; Agid, Y.; Javoyagid, F.; Jenner, P.; Marsden, C. D. *Ann. Neurol.* **1994**, *36*, 348−355.
(62) Rice, M. E.; Russo-Menna, I. *Neuroscience* **1998**, *82*, 1213−1223.
(63) Jiang, J.; Nadas, I. A.; Kim, M. A.; Franz, K. *J. Inorg. Chem.* **2005**, *44*, 9787−9794.
(64) Rubino, J. T.; Riggs-Gelasco, P.; Franz, K. J. *J. Biol. Inorg. Chem.* **2010**, *15*, 1033−1049.
(65) Zelazowski, A. J.; Gasyna, Z.; Stillman, M. J. *J. Biol. Chem.* **1989**, *264*, 17091−17099.
(66) Bofill, R.; Palácios, O.; Capdevila, M.; Cols, N.; González-Duarte, R.; Atrian, S.; González-Duarte, P. *J. Inorg. Biochem.* **1999**, *73*, 57−64.
(67) Palacios, O.; Polec-Pawlak, K.; Lobinski, R.; Capdevila, M.; Gonzalez-Duarte, P. *J. Biol. Inorg. Chem.* **2003**, *8*, 831−842.
(68) Kau, L. S.; Spira-Solomon, D. J.; Penner-Hahn, J. E.; Hodgson, K. O.; Solomon, E. I. *J. Am. Chem. Soc.* **1987**, *109*, 6433−6442.